Improved Intrapulse Raman Scattering Control via Asymmetric Airy Pulses

Yi Hu,[1,2] Amirhossein Tehranchi,[2,†] Stefan Wabnitz,[3] Raman Kashyap,[4] Zhigang Chen,[1,5] and Roberto Morandotti[2,*]

[1]*The MOE Key Laboratory of Weak-Light Nonlinear Photonics, TEDA Applied Physics Institute and School of Physics,*
Nankai University, Tianjin 300457, China
[2]*INRS-EMT, 1650 Boulevard Lionel-Boulet, Varennes, Québec J3X 1S2, Canada*
[3]*Dipartimento di Ingegneria dell'Informazione, Università di Brescia, Via Branze 38, 25123 Brescia, Italy*
[4]*Advanced Photonics Concepts Laboratory, Department of Electrical Engineering and Department of Engineering Physics,*
Ecole Polytechnique, University of Montreal, C.P. 6079, Succursale Centre-ville, Montreal, Québec H3C 3A7, Canada
[5]*Department of Physics and Astronomy, San Francisco State University, San Francisco, California 94132, USA*
(Received 26 June 2014; published 20 February 2015)

We experimentally demonstrate the possibility of tuning the frequency of a laser pulse via the use of an Airy pulse-seeded soliton self-frequency shift. The intrinsically asymmetric nature of Airy pulses, typically featured by either leading or trailing oscillatory tails (relatively to the main lobe), is revealed through the nonlinear generation of both a primary and a secondary Raman soliton self-frequency shift, a phenomenon which is driven by the soliton fission processes. The resulting frequency shift can be carefully controlled by using time-reversed Airy pulses or, alternatively, by applying an offset to the cubic phase modulation used to generate the pulses. When compared with the use of conventional chirped Gaussian pulses, our technique brings about unique advantages in terms of both efficient frequency tuning and feasibility, along with the generation and control of multicolor Raman solitons with enhanced tunability. Our theoretical analysis agrees well with our experimental observations.

Airy pulses are ubiquitous in dispersive optical systems. Such pulses, whose temporal field envelope is described by an Airy function, can be formed by virtue of a cubic spectral phase imposed via either third order dispersion [1] or a pulse shaper. Their asymmetric pulse profiles lead to a variety of applications such as the generation of broadband spectra [2] and coherent control [3]. Airy pulses have attracted increasing attention since their unique dynamics including dispersion-free propagation and self-healing was uncovered in optics [4], finding inspiration from the world of quantum mechanics [5]. As a result, it has been possible, for example, to construct linear spatiotemporal optical bullets [6]. Extensive theoretical and numerical studies have been devoted to the study of the linear and nonlinear dynamics of these pulses under second and/or third order dispersion with or without the presence of a Kerr non-linearity [7,8], as well as to the understanding of their interaction with solitons [9]. However, the experimental investigation of Airy pulses, with a view to elucidate their advantages with respect to conventional Gaussian-based pulses, is still relatively unexplored. The peculiar feature of Airy pulses is that their linear dynamics is exactly coded on their spectral phase, i.e., the cubic term [10], a feature that introduces additional controlling freedom. Nevertheless, such control is rarely applied in a practical framework, particularly under the influence of the higher order non-linearities commonly seen in fiber or integrated optics [11,12]. Among those nonlinearities, stimulated Raman scattering (SRS) is the most fundamental, as it may play a critical role in many of the nonlinear phenomena occurring

in fibers or waveguides. SRS brings asymmetric (in time) pulse dynamics strongly related to its temporally retarded nonlinear response, which enables a continuous downshift of the carrier frequency of a decelerating fundamental optical soliton—or, in other terms, a soliton self-frequency shift (SSFS) [13]. Since Airy pulses exhibit asymmetric temporal shapes, they may show versatile behaviors when paired with the (intrinsically) asymmetric Raman response. For example, Airy or Airy-like beams [4,14,15] have been investigated under the effect of a nonsymmetric (in space) diffusion effect in a photorefractive crystal [16] or under the nonsymmetric boundary condition induced by a highly nonlocal nonlinearity [17]. Moreover, exploiting these pulses in conjunction with SRS will not only be beneficial toward controlling the SSFSs but may also pave the way toward improving existing applications [2,3,11] or even open up new opportunities for controlling other nonlinear phenomena, such as four wave mixing and coherent anti-Stokes Raman scattering.

In this Letter, we study the SSFS initiated by suitably preshaped Airy pulses in fibers. The Airy asymmetric features are not only shown by the overall shape exhibiting a decaying oscillatory tail but also by the asymmetric main lobe. Therefore, under the influence of the (delayed) Raman response, the generation of Raman solitons from the main lobe and their subsequent interaction with the Airy tails behave quite differently depending on whether the Airy pulses are featured by a leading or a trailing tail. In our experiments, we propose a convenient way to control the SSFS by means of a suitable linear chirp applied to the

pulse. Such a prechirp is imposed at the input for both tail-leading and trailing Airy pulses, and the results are compared with the case of a prechirped Gaussian-like pulse, showing significant advantages. Finally, we also discuss how Airy pulses may enable the generation and control of multicolor Raman solitons.

In Fig. 1(a), we present a typical Airy pulse with an oscillating tail in its fast edge. The associated main lobe has an asymmetric shape, exhibiting a peak power value at the time $t = t_p$. In practice, the most convenient and feasible way to generate ultrashort Airy pulses is by modulating the spectrum of a transform-limited pulse through a cubic spectral phase, i.e., $\exp[i(f - f_0)^3/(3\sigma^3)]$, where f is the frequency, f_0 is the center frequency, and σ measures the modulation depth, with a positive (negative) value corresponding to tail-trailing (leading) Airy pulses, respectively. The parameter σ also controls the degree of asymmetry of the main lobe. Providing that A_{main} is defined by the fraction of the power in the main lobe at $t < t_p$ and assuming a Gaussian-shaped spectrum, one can estimate that the value of A_{main} should be in the range between 0.4 and 0.5, where the lower limit corresponds to an infinite Airy pulse while the upper one belongs to the case of a time symmetric Gaussian pulse. Once the overall shape of the Airy pulses is taken into account, a larger asymmetry degree can be introduced, particularly by employing an additional linear chirp, as shown in Fig. 1(b), where the Airy tails merge into the main lobe. Such a chirp can be simply and proportionally obtained by offsetting the cubic phase term by the quantity f_d, through the term $\exp[i(f - f_0 - f_d)^3/(3\sigma^3)]$. In this way, a quadratic spectral phase modulation equal to $\exp(iCf^2)$, where the linear chirp parameter $C = -f_d/\sigma^3$, is equivalently introduced. The degree of temporal asymmetry (now redefined in terms of the fraction of the power in the whole pulse at $t < t_p$ and labeled as A_{whole}) can reach values above 80%, and its range of variation is also increased, e.g., between 0.5 and 0.9 in the case of a 4-nm bandwidth spectrum with a cubic phase of $\sigma = -0.2$ THz, as is shown in Fig. 1(c). Different
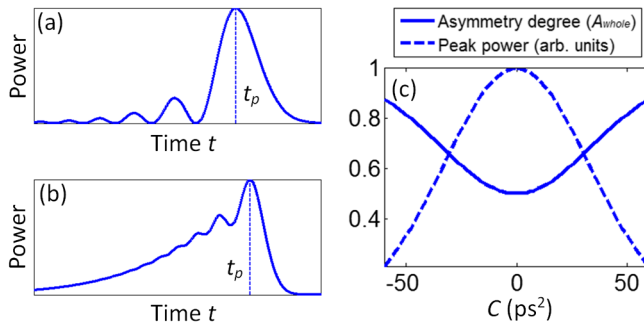
values of the bandwidth or σ are expected to give similar results because of the scaling properties of Airy pulses.

The generalized nonlinear Schrödinger equation [18] was employed to analyze the propagation of Airy pulses in a large effective area fiber (LEAF) (see Methods in Ref. [19]). Figures 2(a) and 2(b) show typical examples of the nonlinear propagation of two time-reversed Airy pulses from numerical simulations with parameters that exactly match the experiments that follow. For such a tail-leading Airy pulse [whose main lobe has a fast leading edge and a slow trailing edge; see Fig. 1(a)], the first generated Raman soliton captures a significant amount of energy due to its relatively longer interaction with the main lobe, a fact that hampers the possibility of generating a secondary Raman soliton [Fig. 2(a)]. Furthermore, the generated soliton continuously slows down upon propagation, and it never meets the input oscillatory Airy tail. In this case, the SSFS process is mostly influenced by the main input lobe. If we now consider the case of a tail-trailing Airy pulse, the first Raman soliton experiences a shorter interaction with the main lobe [Fig. 2(b)], thus gaining less energy, which allows the generation of a secondary Raman soliton, excited by the remainder of the input Airy pulse. Besides the influence that is exerted by the main lobe, the Raman soliton in Fig. 2(b) will eventually overlap with the Airy tail and thus gain further energy by means of their nonlinear interaction [20]. The simulated output spectra for a 625-m-long fiber are shown in Figs. 2(c) and 2(d) for a cubic phase with $|\sigma| = 0.2$ THz, also revealing the secondary Raman soliton generated in the presence of a tail-trailing Airy pulse.

In order to confirm our simulations, we performed the experiment using the setup described in Ref. [10], where a pulse from a fiber laser successively passes through a wave shaper and an amplifier. Besides, a fiber-based polarizer, a 10/90 coupler, and a power meter were employed to make sure that the polarization and the average power of the pulse with a 4-nm bandwidth are always the same at the input of a LEAF fiber spool (from Corning, 625 m long). Figures 2(e) and 2(f) plot the measured output spectra. The secondary Raman soliton generation is evident for the tail-trailing case, but it is suppressed for the tail-leading case, a fact which agrees well with our numerical simulations, although some unavoidable discrepancies caused by the propagation of the pulses from the fiber laser into the wave shaper and amplifier are certainly present. Such a difference associated with the secondary Raman soliton generation is more pronounced for longer propagation distances (see the additional measurements presented in Ref. [19] and Fig. 3). On the contrary, the SSFS associated with the primary Raman soliton for the tail-trailing Airy pulse is relatively smaller, indicating that less power is consumed in the main lobe, also in agreement with our expectation. However, additional and somehow surprising experimental evidence shows that the primary Raman SSFS can also be
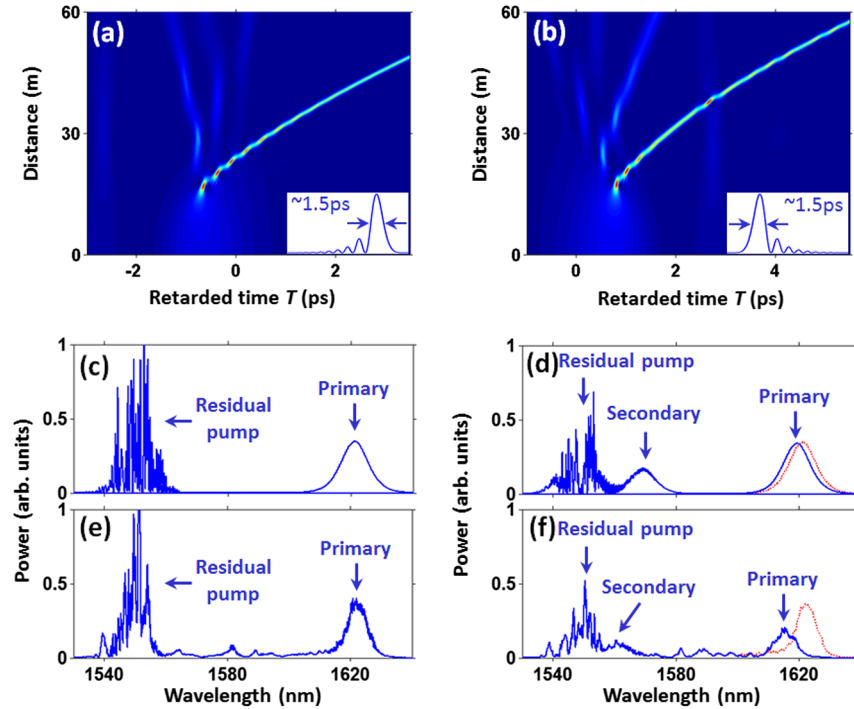

FIG. 1 (color online). (a),(b) The typical shape of a nonchirped and a chirped Airy pulse, respectively. (c) Asymmetry degree (A_{whole}) and peak power for the Airy pulse shown in (a) resulting from different linear chirps, where C is a chirp parameter defined in the text.

FIG. 2 (color online).   Theoretical (a-d) and experimental (e-f) results showing the SSFSs associated with tail-leading (left) and tail-trailing (right) asymmetric Airy pulses. (a),(b) The nonlinear propagation and the insets plot the profiles of the inputs for each case. (c)–(f) The simulated and the experimental output spectra, for both input Airy pulses propagating along a 625-m-long LEAF fiber. The dotted red curves in (d) and (f) are the copies of the corresponding primary SSFS from (c) and (e), allowing for a better comparison between the two cases.

larger if proper (i.e., longer) Airy tails are employed, as a result of a larger energy transfer via the nonlinear interaction.

While these results are certainly interesting on a fundamental point of view, the most important consequences come in terms of applications, such as the improvement of the performance of fiber Raman amplifiers [21] and the implementation of novel spectroscopy sources. Up to date, Gaussian-like input pulses are typically used to induce frequency conversion via the SSFS by employing a linear chirp [22].

In what follows, we propose to use a similar method to obtain tunable SSFS via Airy pulses. The peak power of an Airy pulse at the input can be typically adjusted by altering the offset, as shown in Fig. 1(c). In order to obtain a quite large frequency shift, particularly for the secondary Raman soliton, a longer LEAF fiber spool (6 km) is employed. In the first set of experiments, we use a cubic phase with $\sigma = -0.2$ THz to produce an Airy pulse with a leading oscillatory edge. The average input power was set at 18 mW. By altering the offset f_d of the cubic phase, different SSFSs could be obtained, as shown in Fig. 3(a), where the whole pattern is almost symmetric with respect to the linear chirp C: larger SSFSs are obtained for larger peak powers related to the values of C of Fig. 1(c). Near the region where $C = 0$, it is relatively difficult to generate additional solitons, since the first soliton consumes a

significant amount of energy from the main input lobe. The secondary Raman soliton appearing for large values of C is caused by the merging of the main lobe with the sublobes, as shown in Fig. 1(b). Therefore, the dynamics of such a chirped Airy pulse is similar to that reported in Fig. 2(b) for the tail-trailing Airy pulse. Unlike the primary Raman soliton, the secondary one can now shift to longer wavelengths when C is set further away from 0, as the asymmetric shape tends to allow more power involved in the secondary soliton fission process. Eventually, the frequency shift of the secondary soliton will decrease with increasing C, as a result of a longer input pulse duration (in turn leading to a lower peak power).

Next, we changed the sign of σ and performed another set of experiments for a pulse featuring a trailing tail. The corresponding results are summarized in Fig. 3(b). With the same input average power as before (18 mW), two Raman solitons (primary and secondary) are now clearly emerging for a large range of offsets, in agreement with our predictions. Contrary to the previous case (i.e., an Airy pulse with a leading tail), the dependence of the primary SSFS on the chirping parameter C is of nonsmooth nature. In the experiments, the nonlinear interaction between the Raman soliton and the trailing tails may not be perfectly symmetric with respect to the parameter C, owing to the nonideality of the experimentally generated Airy pulses (as a consequence of the noise introduced by the setup).
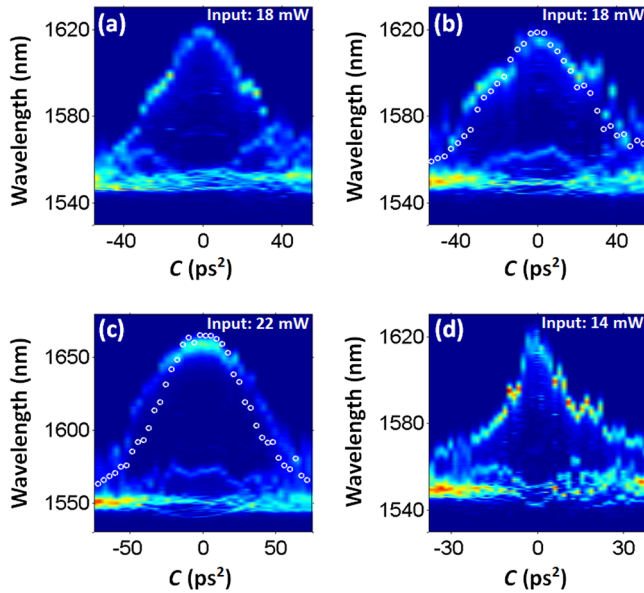
FIG. 3 (color online). Experimental observations of the dependence of the Raman soliton self-frequency shift upon the linear prechirp coefficient C, obtained by using (a) a tail-leading and (b),(c) a tail-trailing Airy pulse, respectively, for different input powers. In (d), a Gaussian-like pulse is presented for comparison. Each spectral pattern is obtained by imposing different linear chirps at the input. The white circles in (b) and (c) trace out the peak of the primary SSFS of tail-leading Airy pulses for 18- and 22-mW input powers, respectively.

Therefore, fluctuations appear on the spectral pattern. The "smoothness" of the SSFS dependence on C, an important parameter toward practical applications, can be improved by using a larger input average power, e.g., 22 mW, as shown in Fig. 3(c). From these two results, one can infer that the energy gain from the Airy tails could be comparable with the one directly extracted from the main lobe in the lower power level case. Moreover, this gain is effectively able to slow down the decay of the SSFS, which would otherwise follow from the decrease in the input peak

power. Therefore, the pattern in Fig. 3(b) looks slightly broader and flatter than that of Fig. 3(a). Such an effect is more apparent for higher input powers [Fig. 3(c)].

Let us consider now the standard case of a Gaussian pulse. Here, we directly use a linear chirp, i.e., $\exp(iCf^2)$, to modulate the input pulse for a suitable frequency tuning. In practice, *different* quadratic phases have to be imposed to induce different degrees of chirp C. Such a process is clearly much more cumbersome if compared to the simple method previously proposed (shift of the cubic phase applied to Airy pulses in function of frequency). Moreover, the nearly transform-limited symmetric pulse is affected by dispersion, thus leading to a narrower shape of the frequency-tuning pattern [Fig. 3(d)] than that presented in Figs. 3(a) and 3(b). In addition, the frequency tuning in Fig. 3(d) is not as smooth as the one in Fig. 3(a). This is due to the fact that the pulse is basically associated with the overall spectrum, rather than with a fraction of it, as is the case for the main lobe of an Airy pulse [23], which thus makes it more susceptible to inhomogeneities or noiselike fluctuations of the spectrum.

From the results above, one can also envisage the possibility to generate and control multicolor Raman solitons, which could lead to a useful light source for fluorescence microscopy [24], on top of possible telecom applications. For example, two Raman solitons can be simultaneously obtained by using the tail-trailing Airy pulse around $C = 0$. The wavelength of these pulses can be tuned by varying the input power, as shown in Fig. 4(a). However, since the secondary soliton is generated from a relatively small portion of the main lobe for both the chirped and nonchirped cases, as inferred from Fig. 1(c), the wavelength difference between the secondary and primary solitons always remains large. Fortunately, by employing chirped tail-leading Airy pulses, it is possible to reduce this wavelength difference by exploiting a larger input asymmetry, as shown in Fig. 1(c). Considering, for instance, a linear chirp around $C = 27$ ps^2 with a cubic phase of $\sigma = -0.2$ THz, the frequency shift as a function of
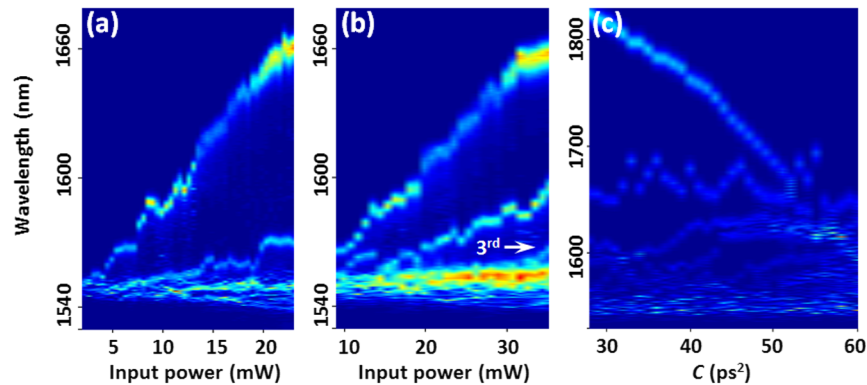

FIG. 4 (color online). (a),(b) Experimental results showing the power-dependent control of multicolor Raman soliton generation via the use of (a) a nonchirped tail-trailing Airy pulse and of (b) a chirped tail-leading Airy pulse. (c) Simulation results showing SSFS tuning obtained by applying a linear chirp C to the tail-leading Airy pulse.

the input power is presented in Fig. 4(b), where the two Raman shifts become closer in wavelength and a third one starts to appear for an input power of 35 mW. Indeed, more than two Raman solitons can be controlled in this way. Figure 4(c) shows a numerical example corresponding to the generation of multicolor Raman solitons from a tail-leading Airy pulse (in the case of a sufficiently high input power), where it is possible to tune the frequency spacing among the solitons by simply altering the offset of the cubic phase.

In conclusion, we have demonstrated the effective control of SSFS and multicolor Raman soliton generation via the use of Airy pulses in fibers. The different dynamics of two inputs with time-reversed shapes are discussed. We found that on the one hand, Raman solitons are chiefly influenced by the main lobe for the tail-leading Airy pulses, while on the other hand, they tend to gain energy from the subsequent interaction with the Airy tails in the case of a tail-trailing pulse. We also note that the generation of a secondary Raman soliton is more difficult in the first case. In our experiment, we proposed a complementary approach to control the Raman frequency shift by altering the offset of the cubic phase applied to the pulses. In addition, we demonstrated the possibility to employ the offset for controlling the spectral position of multicolor Raman solitons in the case of tail-leading Airy pulses. The frequency change as a function of the linear chirp for Airy pulses has advantages in terms of both feasibility and tuning when compared to the use of standard time symmetric Gaussian-like pulses, leading to a smoother control of the frequency shift. Finally, our method can also be applied for investigating the dynamics of other kinds of self-accelerating pulses that can be conveniently engineered through changing the spectral phase and amplitude [23]. These studies will bring about new possibilities for effective frequency tuning of Raman solitons, an important property toward practical application for a host of key technologies ranging from optical communications, metrology, and spectroscopy to biophotonics, and may also promote the studies of Airy or Airy-like pulses in other nonlinear optical systems.

[*]morandotti@emt.inrs.ca
[†]tehranchi@emt.inrs.ca

[1] M. Miyagi and S. Nishida, Appl. Opt. **18**, 2237 (1979).
[2] S. Xu, D. Reitze, and R. Windeler, Opt. Express **12**, 4731 (2004); D. Castelló-Lurbe, E. Silvestre, P. Andrés, and V. Torres-Company, Opt. Lett. **37**, 2757 (2012).
[3] B. Chatel, J. Degert, and B. Girard, Phys. Rev. A **70**, 053414 (2004); V. V. Lozovoy and M. Dantus, ChemPhysChem **6**, 1970 (2005).
[4] G. A. Siviloglou and D. N. Christodoulides, Opt. Lett. **32**, 979 (2007).
[5] M. V. Berry and N. L. Balazs, Am. J. Phys. **47**, 264 (1979).
[6] A. Chong, W. H. Renninger, D. N. Christodoulides, and F. W. Wise, Nat. Photonics **4**, 103 (2010); D. Abdollahpour, S. Suntsov, D. G. Papazoglou, and S. Tzortzakis, Phys. Rev. Lett. **105**, 253901 (2010).
[7] Y. Kaganovsky and E. Heyman, J. Opt. Soc. Am. A **28**, 1243 (2011); Y. Fattal, A. Rudnick, and D. M. Marom, Opt. Express **19**, 17298 (2011); M. A. Preciado, Opt. Express **21**, 13394 (2013).
[8] I. M. Besieris and A. M. Shaarawi, Phys. Rev. E **78**, 046605 (2008); I. Kaminer, Y. Lumer, M. Segev, and D. N. Christodoulides, Opt. Express **19**, 23132 (2011); R. Driben, Y. Hu, Z. Chen, B. A. Malomed, and R. Morandotti, Opt. Lett. **38**, 2499 (2013); R. Driben and T. Meier, Phys. Rev. A **89**, 043817 (2014).
[9] A. Rudnick and D. M. Marom, Opt. Express **19**, 25570 (2011); W. Caia, M. S. Mills, D. N. Christodoulides, and S. Wen, Opt. Commun. **316**, 127 (2014).
[10] Y. Hu, M. Li, D. Bongiovanni, M. Clerici, J. Yao, Z. Chen, J. Azaña, and R. Morandotti, Opt. Lett. **38**, 380 (2013).
[11] C. Ament, P. Polynkin, and J. V. Moloney, Phys. Rev. Lett. **107**, 243901 (2011).
[12] L. Zhang, J. Zhang, Y. Chen, A. Liu, and G. Liu, J. Opt. Soc. Am. B **31**, 889 (2014).
[13] F. M. Mitschke and L. F. Mollenauer, Opt. Lett. **11**, 659 (1986).
[14] G. A. Siviloglou, J. Broky, A. Dogariu, and D. N. Christodoulides, Phys. Rev. Lett. **99**, 213901 (2007).
[15] Y. Hu, G. Siviloglou, P. Zhang, N. Efremidis, D. Christodoulides, and Z. Chen, in Nonlinear Photonics and Novel Optical Phenomena, edited by Z. Chen and R. Morandotti (Springer, New York, 2012), Vol. 170, p. 1.
[16] S. Jia, J. Lee, J. W. Fleischer, G. A. Siviloglou, and D. N. Christodoulides, Phys. Rev. Lett. **104**, 253904 (2010); J. Parravicini, P. Minzioni, V. Degiorgio, and E. DelRe, Opt. Lett. **34**, 3908 (2009).
[17] R. Bekenstein and M. Segev, Opt. Express **19**, 23706 (2011).
[18] J. C. Travers, M. H. Frosz, and J. M. Dudley, in Supercontinuum Generation in Optical Fibers, edited by J. M. Dudley and J. R. Taylor (Cambridge University Press, Cambridge, England, 2010), p. 32.
[19] See Supplemental Material at http://link.aps.org/supplemental/10.1103/PhysRevLett.114.073901 for simulation method employed and more detailed measurements.
[20] F. Luan, D. V. Skryabin, A. V. Yulin, and J. C. Knight, Opt. Express **14**, 9844 (2006).
[21] E. M. Dianov, P. V. Mamyshev, A. M. Prokhorov, and D. G. Fursa, JETP Lett. **46**, 482 (1987).
[22] N. Karasawa, K. Tada, and H. Ohmori, IEEE Photonics Technol. Lett. **19**, 1292 (2007).
[23] Y. Hu, D. Bongiovanni, Z. Chen, and R. Morandotti, Phys. Rev. A **88**, 043809 (2013); Opt. Lett. **38**, 3387 (2013).
[24] K. Wang, T. Liu, J. Wu, N. G. Horton, C. P. Lin, and C. Xu, Biomed. Opt. Express **3**, 1972 (2012).